

Evaluation of Face Image Quality Metrics in Person Identification Problem

Vladimir Khryashchev, Ilya Nenakhov, Anton Lebedev, Andrey Priorov
 P.G. Demidov Yaroslavl State University
 Yaroslavl, Russia
 vhr@yandex.ru, {zergoodsound,lebedevdes}@gmail.com, andcat@yandex.ru

Abstract—Face quality assessment algorithms play an important role in improving face recognition accuracy and increasing computational efficiency of biometric systems. In the case of video analysis system, it is very common to acquire multiple face images of a single person. Strategy for optimally choose of the face images with the best quality from the set of images should base on special quality metric. A set of face image quality metrics were investigated: image resolution, sharpness, symmetry, blur, measure of symmetry of landmarks points S, quality measure based on learning to rank. A new metric based on no-reference image quality assessment approach is proposed. For all the metrics the Spearman rank correlation coefficients with subjective expert assessment at different levels of face image scene illumination were calculated. The received results can help computer vision system engineers to optimize the biometric identification system.

quality evaluation module increase throughput of the surveillance system.

There are several standards that determine the face image quality - ISO/IEC 19794-5, ICAO 9303 [14], [15]. They contain a description of the characteristics that influence the decision on the suitability of the image for the automatic recognition systems. All standardized characteristics are grouped into two classes: the texture (sharpness, contrast and light intensity, compression ratio, other distortions), and characteristics directly related to the face features (symmetry, position, rotation, eyes visibility, the presence of glare or shadows on the face). For their automatic detection, scientific literature describes the following methods - determination of posture [3], [15], illumination and rotation [14],[16].

I. INTRODUCTION

Usually when a person is in front of surveillance video camera several images of his face are saved to a storage. Most of them are useless for the biometric identification system due to several reasons: human's movement leads to blurring, a person can be in the low-light conditions, only a part of the face or significantly turned face may be recorded. Human identification algorithms computationally are complex enough, so recognition of the entire sequence of images can slow down the work of video surveillance systems [1], [2]. Thus, the problem of choosing images of best quality from an all received images by which identification of the person will be performed is important.

The problem is commonly touched in modern scientific literature [3-10]. One of the first approaches to solve this problem is a method based on the application of clustering algorithm according to K-means approach [11]. Practical experiments have shown that it has low accuracy when there are many low quality faces in the received sequence. A totally different approach searches the best quality images for face recognition by making quality evaluation of all images [2], [6]. Typical recognition system with face image quality evaluation module schema is shown in Fig. 1. The quality of face images is estimated at the pre-processing stage. Low quality images are removed or archived, the recognition applies only to high-quality images. It is shown in [2] that the use of face image

quality evaluation module increase throughput of the surveillance system.

There is a group of face image quality assessment algorithms that uses objective methods to determine standardized facial quality characteristics. Overall facial image quality is obtained by combining the results of these methods. This group of algorithms is called metric fusion algorithms. The metric fusion can be done by thresholding each of characteristic value. In this case, residual quality would be a number of characteristics above threshold. Another approach of metric fusion assigns a weight to every measured standardized characteristic [9]. Machine learning methods are widely used to determine metrics weights. It should be noted that metric fusion algorithms are tied to a specific database of training images, as well as to a specific recognition system. To solve this problem, a fundamentally different approach for measuring facial image quality, without using standardized facial quality characteristics(ex. a statistical method based on the face model [6] or the method based on the learning to rank [7]) was created.

In none of the available papers expert evaluation of face image quality were used. At the same time, expert opinions are widely applied in the analysis of images and video sequences quality [17], [23]. It should be noted that human could easily identify the most of standardized facial image quality characteristics.

The aim of this paper is to investigate a set of face images quality metrics in the face identification problem and compare the receiving results with the same expert evaluation.

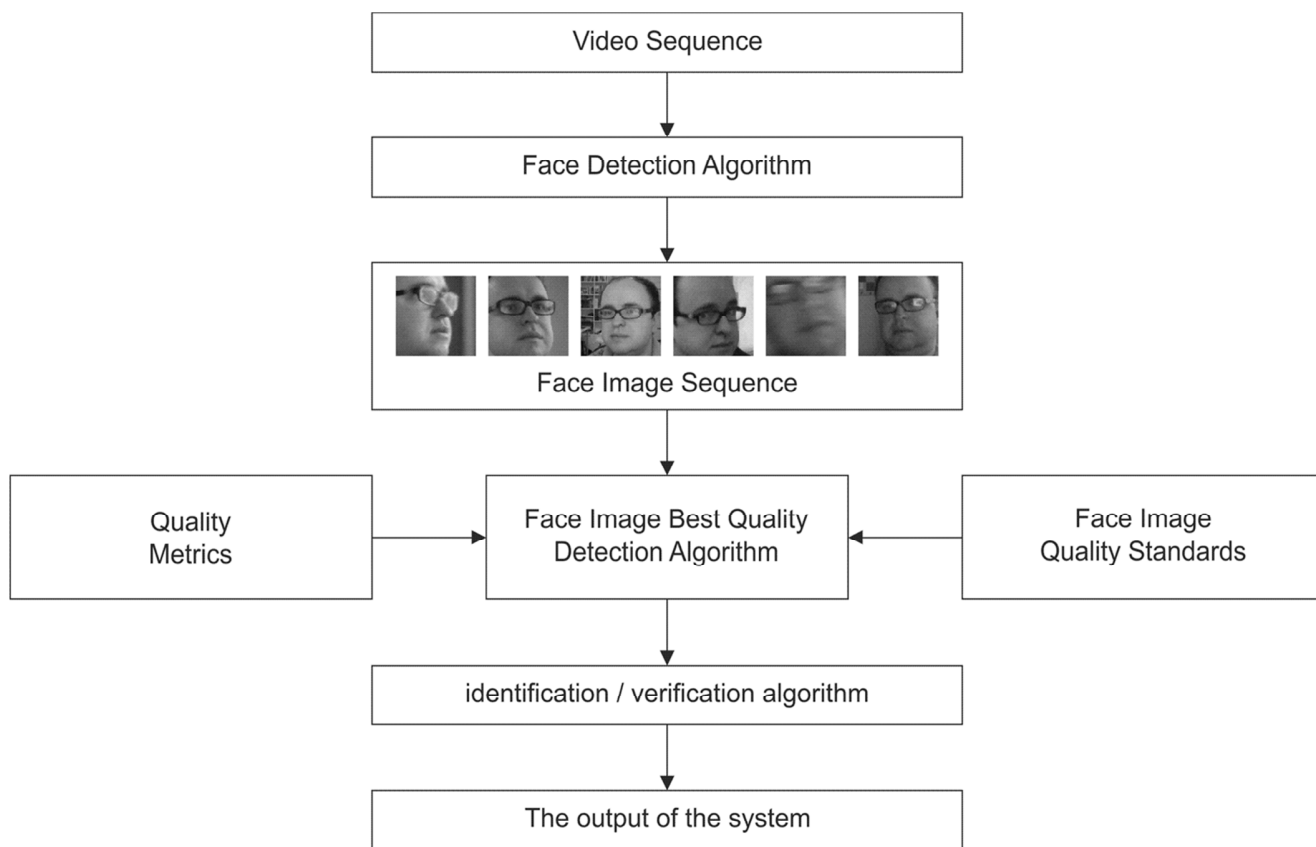


Fig. 1. Recognition system with face image quality evaluation module

II. DESCRIPTION OF INVESTIGATED METRICS

A. No-reference image quality assessment algorithm (NRQ LBP)

No-reference image quality assessment has gained considerable importance in the last decade [17], [23]. To use such algorithm in a face quality assessment task we need to ensure that this algorithm is fast enough to perform in near “real-time” mode. There are two no-reference image quality assessment algorithms which operate in spatial domain and could be candidates to use them for texture quality measurement of facial image. These algorithms are NRQ LBP and BRISQUE.

The NRQ LBP algorithm contains two steps. First is the quality feature extraction step. Features are local binary patterns with neighborhood radiuses 1, 2, 3 pixels. Second is the mapping step. Here extracted features are mapped with subjective DMOS score. For mapping machine learning algorithm “Extra Trees Regressor” is used [20]. The output value of NRQ LBP algorithm is in range from 0 to 100, because features are mapped to DMOS scores. The smaller the output value the better the result image quality is.

Local binary pattern (LBP) is a binary code which describes the pixel’s neighborhood. Parameter r is the neighborhood radius. Parameter P is a number of pixels in the neighborhood (Fig. 2).

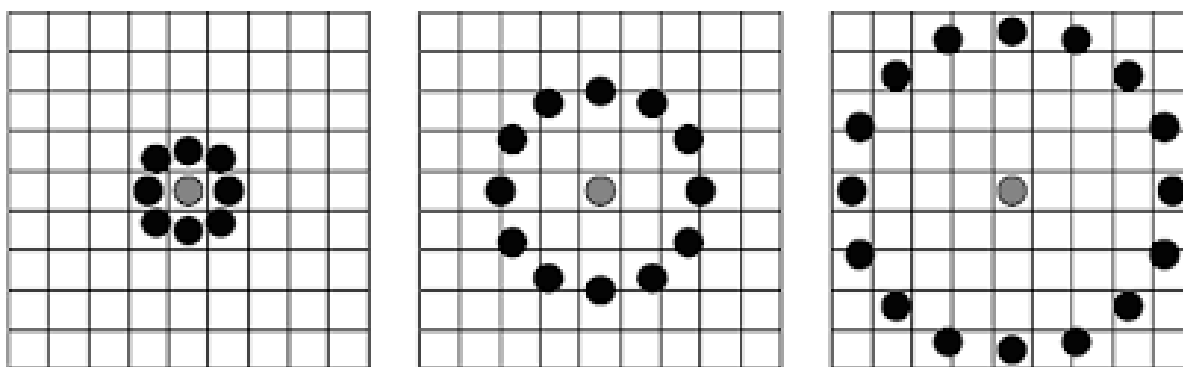


Fig. 2. The circular neighborhoods with appropriate (P, r) values (8, 1), (12, 2), (16, 4)

Consider image I and let g_c be the luminance value of central pixel with (x, y) coordinates. Central pixel is the pixel for which the LBP binary code is computed. The following is used for choosing pixels from neighborhood:

$$g_p = I(x_p, y_p), \quad p = 0, \dots, P-1. \quad (1)$$

$$x_p = x + R \cos\left(\frac{2\pi p}{P}\right), \quad (2)$$

$$y_p = y - R \sin\left(\frac{2\pi p}{P}\right), \quad (3)$$

where g_p – luminance value of the neighborhood pixel, x_p and y_p – it's coordinates. Bilinear interpolation is used when the sampling point is not in the center of a pixel. The value of a luminance of the central pixel is the threshold. If luminance value of pixel from neighborhood is more than the threshold then 1 is set in the appropriate place of the binary code 0 is set otherwise.

Formally, LBP can be described as follows:

$$LBP_{p,r} = \sum_{p=0}^{P-1} S(t_i - t_c) 2^p, \quad (4)$$

$$S(t) = \begin{cases} 1, & t \geq 0 \\ 0, & t < 0 \end{cases}, \quad (5)$$

where t_c – luminance value of the central pixel, t_i - luminance value of the neighborhood pixel, P – number of neighborhood pixels. The output of the LBP function is a binary code which describes pixel's neighborhood.

Local binary pattern is called “uniform” if it contains number of bit-wise transitions from 0 to 1 and vice versa less than 2, for example patterns 0000011, 00111000 are uniform and pattern 01010010 is not. In average 90% of all calculated patterns are uniform [21]. In uniform LBP mapping there is a separate output label for each uniform pattern and all the non-uniform patterns are assigned to a single label. The number of different uniform patterns for code length p is $p(p+1)+3$ while the number of non-uniform patterns is 2^p , so we can save resources working only with uniform patterns.

Then local binary patterns are calculated for all pixels in the image and the histogram H is built:

$$H(k) = \sum_{m=1}^M \sum_{n=1}^N f(LBP(m, n), k), \quad k \in [0, K], \quad (6)$$

$$f(x, y) = \begin{cases} 1, & x = y \\ 0, & x \neq y \end{cases}, \quad (7)$$

where k – number of patterns [22]. We use rotation invariant local binary patterns as quality features. Rotation invariant means that patterns that can be obtained from each other by

circle shift are placed into one histogram bin. As it was said above, we calculate features for multiple neighborhood radiuses 1, 2, 3, so as a result we have 54 quality features for a particular image.

B. BRISQUE

BRISQUE is an algorithm for no-reference image quality assessment in a spatial domain. It contains 2 main stages – feature extraction and mapping. The output from a first stage is a feature vector, which is mapped to subjective quality score (DMOS) during a second stage. This mapping is achieved by solving a regression task. This part is generic enough to allow for the use of any regressor for solving it. In original implementation, a support vector machine regressor is used.

BRISQUE algorithm uses the fact that mean subtracted contrast normalized (MSCN) coefficients strongly tend towards a unit normal Gaussian characteristic. In [23] it is shown that, each distortion modifies the statistics of MSCN in its own way and there are regularities between a distortion type and a statistics variation. For example, blur creates a more Laplacian appearance, while white-noise distortion appears to reduce the weight of the tail of the histogram.

Generalized Gaussian distribution (GGD) can be used to effectively capture a broader spectrum of distorted image statistics:

$$f(x; \alpha, \sigma^2) = \frac{\alpha}{2\beta\Gamma(1/\alpha)} \exp\left(-\frac{|x|^\alpha}{\beta}\right), \quad (8)$$

$$\beta = \sigma \sqrt{\frac{\Gamma(1/\alpha)}{\Gamma(3/\alpha)}}, \quad (9)$$

$$\Gamma(\alpha) = \int_0^\infty t^{\alpha-1} e^{-t} dt \quad \alpha > 0, \quad (10)$$

where α – controls the shape, σ^2 – control the variance.

Values of (α, σ^2) are estimated for the tested image and form a first features set of BRISQUE algorithm. Second feature set is formed from pairwise products of neighboring MSCN coefficients along four orientations – horizontal, vertical, main-diagonal and secondary diagonal.

Pairwise MSCN products for distorted images obey the asymmetric generalized Gaussian distribution:

$$f(x; \nu, \sigma_l^2, \sigma_r^2) = \begin{cases} \frac{\nu}{(\beta_l + \beta_r)\Gamma(1/\nu)} \exp\left(-\left(\frac{-x}{\beta_l}\right)^\nu\right) & x < 0 \\ \frac{\nu}{(\beta_l + \beta_r)\Gamma(1/\nu)} \exp\left(-\left(\frac{-x}{\beta_r}\right)^\nu\right) & x \geq 0 \end{cases}, \quad (11)$$

$$\beta_l = \sigma_l \sqrt{\frac{\Gamma(1/\nu)}{\Gamma(3/\nu)}}, \quad (12)$$

$$\beta_r = \sigma_r \sqrt{\frac{\Gamma(1/\nu)}{\Gamma(3/\nu)}}. \quad (13)$$

BRISQUE second features set contains values of $(\eta, \nu, \sigma_l^2, \sigma_r^2)$, where ν – controls the shape of the distribution, σ_l^2 and σ_r^2 are scale parameters that control the spread on each

side of the mode, respectively. The first parameter from second feature set is calculated as:

$$\eta = (\beta_r - \beta_l) \frac{\Gamma\left(\frac{2}{v}\right)}{\Gamma\left(\frac{1}{v}\right)}. \quad (14)$$

All features are extracted at 2 scales – the original image scale and at a reduced scale (low pass filtered and down sampled by a factor of 2). Thus, a total 36 features are extracted for a tested image.

C. The algorithm based to learning on rank

The disadvantage of the methods described in [2], [4], [6] is the fact that they do not take into account possible differences in recognition algorithms. For example, a recognition algorithm can accurately recognize faces, even if part of the face covered by another object, for example, by hand. For such algorithm faces with occlusion must not have a poor quality, whereas an algorithm which does not work accurately for faces with occlusion, it should be the opposite. Considering the drawbacks of the existing solutions, here an algorithm based on the method of learning to rank is proposed. This algorithm consists of two stages: normalization (with more or less typical) and quality control.

1) *Quality control*: Assume that the face recognition algorithm is tested on the databases A and B , and algorithm based on database A has higher accuracy than the one based on database B . This suggests that for used recognition algorithm, the images from the database A are of better quality than the images from the database B . Let's write it in the form: $A > B$. Two images I_i and I_j are selected from A and B , respectively. The function $f(\cdot)$, which input is image, and the output – a feature vector. Let's define a linear function of image quality $S(I) = w^T f(I)$. The goal to find a vector w that would meet conditions (15-17) as much as possible, and we should consider that images from one database have the same quality image.

$$w^T f(I_i) > w^T f(I_j); \forall I_i \in A, \forall I_j \in B \quad (15)$$

$$w^T f(I_i) > w^T f(I_j); \forall I_i \in A, \forall I_j \in A \quad (16)$$

$$w^T f(I_i) > w^T f(I_j); \forall I_i \in B, \forall I_j \in B \quad (17)$$

The description above matches with the formulas from paper [7], and, respectively, may be represented in the following terms: $\xi_{i,j} \geq 0$, $\eta_{i,j} > 0$, $\gamma_{i,j} \geq 0$

$$\begin{aligned} & \text{minimize} \left(\|w^T\|_2^2 + \lambda_1 \sum \xi_{i,j}^2 + \lambda_2 \sum \eta_{i,j}^2 + \lambda_3 \sum \gamma_{i,j}^2 \right) \\ & w^T (f(I_i) - f(I_j)) \geq 1 - \xi_{i,j}; \forall I_i \in A, \forall I_j \in B \\ & w^T (f(I_i) - f(I_j)) \leq \eta_{i,j}; \forall I_i \in A, \forall I_j \in A \\ & w^T (f(I_i) - f(I_j)) \leq \gamma_{i,j}; \forall I_i \in B, \forall I_j \in B \\ & \xi_{i,j} \geq 0, \quad \eta_{i,j} > 0, \quad \gamma_{i,j} \geq 0 \end{aligned} \quad (18)$$

This approach can be extended to a larger number of databases and features. If a mixture of signs is used, two tier strategy should be used. Assume that m different feature vectors could be extracted from the image I . For i -th vector the quality will be calculated according to the formula $S_i(I) = w_i^T f_i(I)$, ($i = 1, 2, \dots, m$). In the first phase of learning, vector weights w_i are calculated according to the formula (4) for all of the various features. $\vec{S} = [S_1(I), S_2(I), \dots, S_m(I)]^T$ is column vector containing various quality ratings for each attribute respectively. In the author's implementation $m = 5$ is used. Let's define face image quality at step two as $S_k(I) = w_k f_\phi(\vec{S})$, where f_ϕ – polynomial function, which is represented by the expression (19).

$$\begin{aligned} f_\phi(\vec{S}) = & \left[\left(\frac{1}{\sqrt{2}} \right) S_1 S_1^2 (\sqrt{2}) S_2 (\sqrt{2}) S_1 S_2 S_2^2 (\sqrt{2}) S_3 (\sqrt{2}) S_1 S_3 \right. \\ & (\sqrt{2}) S_2 S_3 S_3^2 (\sqrt{2}) S_4 (\sqrt{2}) S_1 S_4 (\sqrt{2}) S_2 S_4 (\sqrt{2}) S_3 S_4 S_4^2 \\ & \left. (\sqrt{2}) S_5 (\sqrt{2}) S_1 S_5 (\sqrt{2}) S_2 S_5 (\sqrt{2}) S_3 S_5 (\sqrt{2}) S_4 S_5 S_5^2 \right] \end{aligned} \quad (19)$$

D. Sharpness

In real life situations, the objects in front of the surveillance camera are not static. That is why the images of these objects may be blurred. The task of defining of the blur degree is one of the most important challenges in quality assessment of face images. The high values of this measure should be assigned to images without blur. Discrete Laplace operator is used to calculate sharpness measure for the image:

$$L(I) = \left| \frac{\partial^2 I}{\partial x^2} \right| + \left| \frac{\partial^2 I}{\partial y^2} \right|. \quad (20)$$

The discrete second derivatives may be computed as convolution with the following kernels: $(1, -2, 1)$ and $(1, -2, 1)^T$. Sharpness estimation is made directly inside face area.

E. Symmetry of landmarks points

Coordinates of the landmarks points obtained by the detector described in [18] are used to determine the symmetry of the face in the image. Each landmark point is numbered from 1 to 68. Only 22 landmarks points with the numbers 9, 31, 32, 36-49, 52, 55, 58, 63, 67 are used. It allows increasing the productivity of the proposed algorithm.

Straight line through the points 9 and 31 is used to determine the degree of deviation from the front face position. Then the distance w between points 37 and 46 is computed. The resulting measure S is calculated according to the following equation:

$$S = \frac{|d_{32} - d_{36}| + |d_{40} - d_{43}| + |d_{37} - d_{46}| + |d_{49} + d_{55}|}{w} + \frac{d_{52} + d_{67}}{w} \quad (21)$$

where d_i is the distance between point i and the straight line described above.

F. Symmetry

Symmetry metric is an assessment of how much the person's current posture is different from frontal and how much inhomogeneous is lighting. In [9] the symmetry of the metric is calculated as the intersection of directed gradients histograms (HoG-descriptors) in symmetric landmarks points of a face:

$$d(i) = \sum_i \min(H_i^L(i), H_i^R(i)) \tag{22}$$

$$Sym = \frac{1}{N} \sum_{i=1}^N d(i), \tag{23}$$

where $H_i^L(i)$ is a calculated function of the oriented gradients histogram at a landmark point with index i . Symmetrically located landmarks points have the same value i , that $H_i^L(i)$ is calculated for the i -th point of the left. Sym is the value of the considered symmetry metrics, and N – number of pairs of landmarks facial points.

III. EXPERIMENTAL RESULTS

Experiments performed on 2 collected databases. First database (Khryashchev Face Comparison Database – KFCD) contains 10 test video sequences for every person recorded at different lightning conditions - 20, 50, 75, 130, 180, 500 lx. Two types of image extracting are used: manual (made by experts) and automatic extraction (every 25th frame is extracted). The samples of such images are presented in Fig. 3 and Fig. 4. Standard face detector [19] is used to detect faces. The following measures are calculated for every detected face: image resolution, sharpness, symmetry, blur, measure of symmetry of landmarks points S , quality measure K (based on learning to rank [7]) and two no-reference image quality metrics NRQ LBP and BRISQUE. In addition, the expert quality assessment has been conducted for each image with values ranging from 1 (worst quality) to 10 (best quality).

The Spearman rank correlation coefficient is used as a similarity score between expert rank and rank for each measure for images with the same illuminance. The resulting values of the Spearman rank correlation coefficient for test images extracted by experts are presented in Table I. The greater value

of the correlation coefficient corresponds to the best correlation between the measure and the expert ratings.

The simulation results show that in conditions of low illuminance levels (<50 lx) the blur measure has the highest correlation coefficient that is caused by the low average quality of relevant video sequences. At normal and high illuminance levels (>130 lx) the proposed measure based on symmetry of landmarks points S outperform other quality measures. Low values of correlation coefficient obtained on some test image datasets (50 and 180 lx) can be explained by the fact that the efficiency of symmetry determining algorithms depends on accuracy rate of detector of landmarks points which decreases with significant face rotation or blur caused by the movement of a person.

The values of correlation coefficient for K measure are low in most cases. The values of K measure often fall within a narrow range of values, for example, a range of values for the test set with the illuminance of 75 lx is equal to 15 units between the worst and the best image quality, although the entire range of measure values is 100 units.

In addition we measure top-3 accuracy for each investigated metric. Top-3 accuracy is the number of matches between 3 top quality images chosen by experts and by objective metrics. Top-1 accuracy is measured similarly. The results presented in Table II show that the better choice of high-quality images is made based on learning to rank K metric. The second position belongs to the proposed symmetry of landmarks points metric S . This result can be explained by the fact that both subjective assessment and S metric are calculated in the spatial domain. The accuracy of the no-reference NRQ LBP metric depends on the luminance level. It performs well when luminance is more than 100 lx.

The second database contains facial images of 60 persons (60 Person Face Comparison Database – 60PFCD) obtained in real-life situation at low lighting conditions (<100lx). There are 10 images for each person Fig. 5. A group of 10 experts defines the best quality image (top1) and the best 3 quality images for each 60 persons. To obtain mean, we weight experts results – every image from top-1 gets weight of 3 other images from top-3 get weight of 2 (no difference between second and third quality images). Like in previous experiments, we compute investigated facial quality metrics scores for each image in the dataset. Tables III-IV contain top-1 accuracy and top-3 accuracy results for objective face quality metrics. It is clear that metric K is more accurate than other investigated metrics.

TABLE I. RANK CORRELATION FOR DIFFERENT FACIAL IMAGE QUALITY METRICS

Illuminance, lx	K	Resolution	Sharpness	S	NRQ LBP	BRISQUE	Symmetry
20	0.02	0.40	-0.17	-0.05	0,25	0,33	0.02
50	0.36	-0.03	0.03	0.05	-0,13	-0,23	0.15
75	-0.37	-0.09	-0.06	-0.15	-0,004	-0,28	0.23
130	0.1	0.36	-0.1	0.45	0,33	0.73	0.28
180	-0.03	-0.09	-0.21	0.06	0,1	-0,25	0.05
500	0.10	-0.15	-0.30	0.28	0.79	-0,06	0.22

TABLE II. TOP-3 ACCURACY OF FACIAL IMAGE QUALITY METRICS (KFCD DATASET)

Illuminance, lx	Presence of glasses	K	Resolution	Sharpness	S	NRQ LBP	BRISQUE	Symmetry
20	-	1	1	1	1	0	0	1
20	+	2	0	2	1	0	2	2
50	-	1	1	1	0	0	0	1
50	+	3	0	0	2	0	1	2
75	-	1	1	0	2	0	1	0
75	+	2	1	1	1	2	1	0
130	-	2	1	1	1	1	0	0
180	-	3	0	1	2	1	0	1
180	+	0	0	0	1	1	1	1
500	+	2	0	0	1	1	0	1
Total		17	5	7	12	6	6	9



Fig. 3. Test images from KFCD dataset with different distortions :a) face rotation; b) blur; c) low resolution of face image

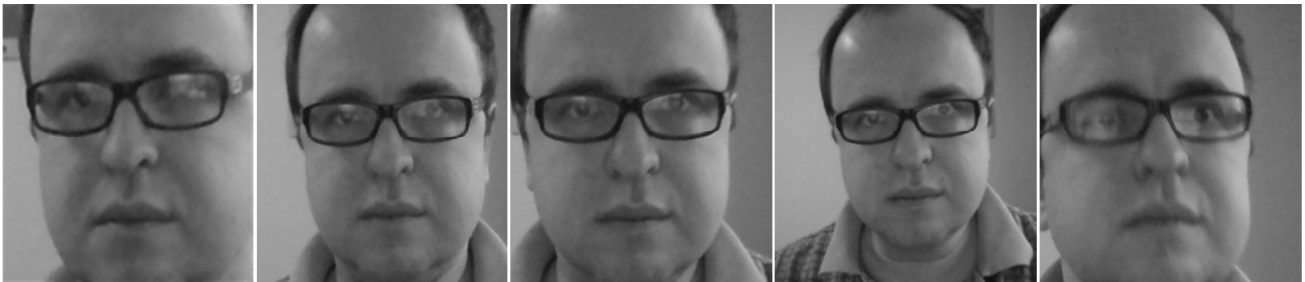


Fig. 4. Test images KFCD dataset extracted automatically (every 25th frame is extracted)

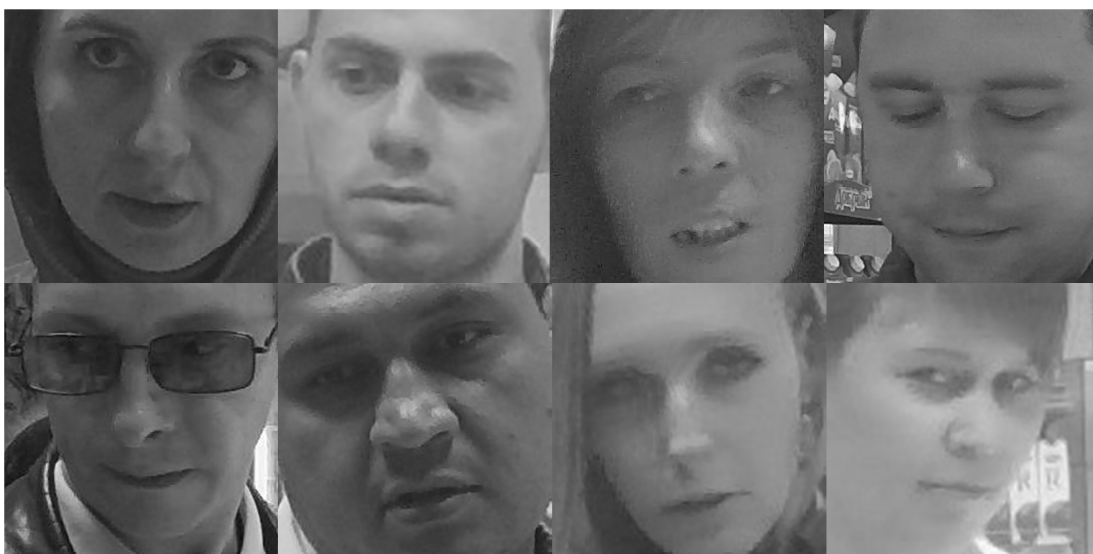




Fig. 5. Facial images from 60PFCD dataset

TABLE III. TOP-1 ACCURACY OF FACIAL IMAGE QUALITY METRICS (60PFCD DATASET)

K	Resolution	Sharpness	S	NRQ LBP	BRISQUE	Symmetry
20	6	7	7	4	7	10

TABLE IV. TOP-3 ACCURACY OF FACIAL IMAGE QUALITY METRICS (60PFCD DATASET)

K	Resolution	Sharpness	S	NRQ LBP	BRISQUE	Symmetry
99	65	60	73	49	52	68

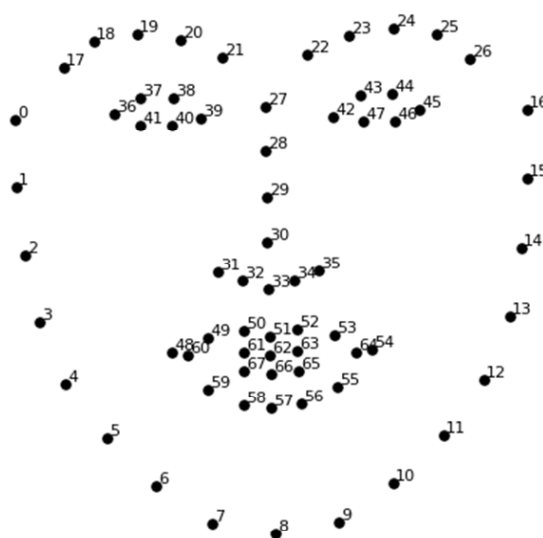


Fig. 6. Landmarks points location diagram

IV. CONCLUSIONS

The investigation of a number of metrics facial image quality. The simulation results show that under low lightning conditions better correlation with subjective expert assessment shows metric blur that is caused by the low average quality of relevant video sequences. In normal and high level of illumination shows the best correlation metric is developed based on the symmetry of the landmarks points.

A set of face image quality metrics were investigated in relation to the problem of selecting the best images for biometric identification. The simulation results show that in conditions of low illuminance levels the blur measure is better correlated to the expert rating that is caused by the low average quality of relevant video sequences. At normal and high illuminance levels the proposed measure based on symmetry of landmarks points outperform other quality measures. In the experiment on a choice of three best pictures the measure based on learning to rank shows the best result. The results will be useful to engineers in building video surveillance and biometric identification using facial image.

ACKNOWLEDGMENT

This work was supported by Russian Foundation for Basic Research grants (№ 15-07-08674 and № 15-08-99639).

REFERENCES

- [1] W. Zhao, R. Chellappa, P. Phillips and A. Rosenfeld, "Face recognition: A literature survey", *ACM Computing Surveys (CSUR)*, vol. 35, № 4, 2003, pp. 399–458.
- [2] N. Ozay, Y. Tong, W. Frederick and X. Liu, "Improving face recognition with a quality-based probabilistic framework", *In Computer Vision and Pattern Recognition (CVPR) Biometrics Workshop*, 2009, pp. 134–141.
- [3] X. Zhu and D. Ramanan, "Face detection, pose estimation and landmark localization in the wild", *Proc. of the IEEE Conference on Computer Vision and Pattern Recognition*, 2012, pp. 2879–2886.
- [4] X. Gao, S. Z. Li, R. Liu and P. Zhang, "Standardization of face image sample quality", *Proc. Int. Conf. Biometrics*, 2007, pp. 242–251.
- [5] K. Nasrollahi and T.B. Moeslund, "Face quality assessment system in video sequences", *BIOID, Lecture Notes in Computer Science (LNCS)*, vol. 5372, 2008, pp. 10–18.
- [6] Y. Wong, S. Chen, S. Mau, C. Sanderson and B.C. Lovell, "Patch-based probabilistic image quality assessment for face selection and

- improved video-based face recognition”, *Computer Vision and Pattern Recognition (CVPR) Workshops*, 2011, pp. 74–81.
- [7] J. Chen, Y. Deng, G. Bai and G. Su, “Face Image quality assessment based on learning to rank”, *IEEE Signal Processing Letters*, vol. 22, № 1, 2015, pp. 90–94.
- [8] J. Chen, C. Yang, Y. Deng, G. Zhang and G. Su, “Exploring facial asymmetry using optical flow”, *IEEE Signal Processing Letters*, vol. 21, № 7, 2014, pp. 792–795.
- [9] M. Nikitin, A. Konushin and V. Konushin, “Face quality assessment for face verification in video”, *Proceedings of GraphiCon'2014*, 2014, pp. 111–114.
- [10] A. Hadid and M. Pietikainen, “From still image to video-based face recognition: An experimental analysis”, *In Proc. Automatic Face and Gesture Recognition (AFGR)*, 2004, pp. 813–818.
- [11] S. Berrani and C. Garcia, “Enhancing face recognition from video sequences using robust statistics”, *In IEEE International Conference on Video and Signal Based Surveillance (AVSS)*, 2005, pp. 324–329.
- [12] ISO/IEC 19794-5 (published version). Information technology – Biometric Data Interchange Formats, 2005.
- [13] Machine readable travel documents. International Civil Aviation Organization, 2006.
- [14] J. Sang, Z. Lei and S. Z. Li, “Face image quality evaluation for ISO/IEC standards 19794-5 and 29794-5”, *In ICB, Lecture Notes in Computer Science (LNCS)*, vol. 5558, 2009, pp. 229–238.
- [15] Z. Yang, H. Ai, B. Wu, S. Lao and L. Cai, “Face pose estimation and its application in video shot selection”, *In International Conference on Pattern Recognition (ICPR)*, 2004, pp. 322–325.
- [16] G. Zhang and Y. Wang, “Asymmetry-based quality assessment of face images”, *In ISVC, Lecture Notes in Computer Science (LNCS)*, vol. 5876, 2009, pp. 499–508.
- [17] I. Nenakhov, V. Khryashchev and A. Priorov, “No-Reference Image Quality Assessment based on Local Binary Patterns”, *Proceedings of the 14th IEEE EAST-WEST DESIGN & TEST SYMPOSIUM*, 2016, pp. 529–532.
- [18] Z. Feng, P. Huber, J. Kittler, W. Christmas, X.J. Wu, “Random cascaded-regression copse for robust facial landmark detection”, *IEEE Signal Processing Letter*, vol. 22, № 1, 2015, pp. 76–80.
- [19] J. Howse. *OpenCV Computer vision with Python*. Birmingham: Packt Publishing Ltd., 2013.
- [20] P. Geurts, D. Ernst and L. Wehenkel, “Extremely randomized trees, Machine Learning”, vol. 36, № 1, 2006, pp. 3–42.
- [21] M. Pietikainen, A. Hadid, G. Zhao and T. Ahonen, *Computer vision using local binary patterns*. Springer, 2011.
- [22] M. Zhang, J. Xie, X. Zhou and H. Fujita, “No reference image quality assessment based on local binary pattern statistics”, *Vis. Commun. Image Process. (VCIP)*, 2013, pp. 1–6.
- [23] A. Mittal, A. Moorthy and A. Bovik, “No-reference image quality assessment in the spatial domain”, *IEEE Trans. Image Process.*, 2012, vol. 7, № 12, pp. 4695–4708.